J Mater Sci (2011) 46:5044–5049
DOI 10.1007/s10853-011-5424-9

Effect of solvents on the dynamic viscoelastic behavior of poly(methyl methacrylate) film prepared by solvent casting

Niranjan Patra · Marco Salerno · Alberto Diaspro · Athanassia Athanassiou

Received: 13 January 2011 / Accepted: 26 February 2011 / Published online: 26 March 2011

Abstract Poly(methyl methacrylate) films were prepared by dissolving the polymer in chloroform, toluene and tetrahydrofuran, with identical concentrations of 200 mg/mL, and drop casting the solutions on Teflon surface at room temperature. The thermal, thermomechanical and structural properties have been investigated by differential scanning calorimetry, dynamic mechanical analyzer, and Fourier transform infrared spectroscopy, respectively. The dynamic mechanical behavior of the films has been measured over a temperature range of 30–150 °C, using sinusoidal stress with a frequency of 2 Hz. The samples prepared from tetrahydrofuran showed the highest storage modulus, indicating a higher polymer chain entanglement in that solvent, whereas the samples prepared from chloroform showed the lowest storage modulus. The samples prepared from chloroform, which showed the weakest mechanical properties, also showed the lowest glass transition temperature, which is evidence of the plasticization and solvent retention mechanism of chloroform. The spectroscopic analysis confirmed the solvent-polymer interactions giving rise to the above mentioned effects.

N. Patra · M. Salerno · A. Diaspro · A. Athanassiou
Italian Institute of Technology, via Morego 30, 16163 Genoa, Italy

N. Patra (✉)
University of Genova, viale Causa 13, 16145 Genoa, Italy
e-mail: niranjan.patra@iit.it

A. Athanassiou
National Nanotechnology Laboratory, CNR—Istituto di Nanoscienze, via Arnesano, 73100 Lecce, Italy

A. Athanassiou
Center for Biomolecular Nanotechnologies of IIT @UniLe, via Barsanti Arnesano, 73010 Lecce, Italy

Introduction

Poly(methyl methacrylate) (PMMA) is a wide spread thermoplastic polymer commonly employed as the main component of positive resists for both electron and UV photo-lithography [1, 2], as well as an imprintable material for soft lithography by hot-embossing [3]. Owing to its excellent transparency in the visible part of the electromagnetic spectrum PMMA is widely used in optical applications especially as a matrix for non-linear optical composite materials, as well as in microelectronics, food packaging, pharmaceutical products, dentistry, and cosmetics [4, 5].

PMMA samples casted from solutions of different solvents have been extensively studied in the literature, in order to elucidate how the solvent affects the polymer. Bistac and Schultz [6] considered the effect of chloroform and toluene on the temperature of the α-relaxation for bulk PMMA and drop casted films, explaining the difference as an acid-base interaction between the basic sites of PMMA and the acidic character of the solvent. Feng et al. [7] applied an ultrasonic field to nascent PMMA films obtained by drop casting, and found that the ultrasonic vibration decreases the amount of residual solvent in the film to one-twelfth of the value which occurs by spontaneous evaporation. Other studies focused on the effect of dimethyl formamide and tetrahydrofuran (THF) on the miscibility in the liquid phase between PMMA and polyvinyl chloride at different relative concentrations [8], and the effect of solvents on the morphology of films prepared by either laser evaporation [9] or drop casting [10].

However, little information is reported in the literature about the thermomechanical behavior of PMMA obtained on solvent evaporation from casted concentrated solutions of PMMA.

In this study, PMMA samples produced from different solvents were investigated experimentally. The studied solvents are chloroform, toluene, and THF, which were selected based on their widespread use. The techniques used for sample characterization were differential scanning calorimetry (DSC), dynamic mechanical analysis (DMA), and Fourier transformed infrared spectroscopy (FTIR), which allowed the examination of thermal (i.e., glass transition temperature), thermomechanical (i.e., storage modulus, loss modulus, creep, and stress relaxation), and structural properties of the samples (i.e., bonding type and occurrence), respectively.

Materials and methods

PMMA of M_w ~120 kg/mol in powder form, toluene, chloroform, and THF of analytical grade were purchased from Sigma-Aldrich (Milan, Italy) and used without further purification. The PMMA powder was first dissolved in three-different solvents considered, with the same PMMA wt/vol concentration of 200 mg/mL. The mixture was shaked at room temperature until the polymer appeared to be completely dissolved and the resulting solution looked optically clear. The PMMA samples for the DMA measurements were prepared by drop casting the PMMA solutions onto clean Teflon surfaces. More precisely, a Teflon sheet of approximately 27×32 mm^2 surface area was completely covered by the solution, by dispensing it until wetting the entire surface. Typically, a solution volume of ~1.3 mL was required to this goal. After drying, the anti-sticking property of Teflon allowed to remove the PMMA film, from which the outer edges were first cut off, and which was then cut into five pieces of approximately 6×12 mm^2 surface area to be used for the DMA measurements. These pieces had a thickness of ~0.25 mm as measured by a digital micrometer (Mitutoyo USA), which did not change significantly on storing them at room temperature for 15 days since preparation for best solvent removal. In the following, the PMMA samples produced from solutions of different solvents will be termed shortly as PMMA/solvent.

The DSC measurements were performed by Pyris Diamond SII (Perkin-Elmer, USA), by scanning the temperature from 20 to 150 °C with a ramping rate of 10 °C/min, operating in a nitrogen atmosphere at a flow rate of 20 mL/min. The DSC instrument was calibrated using indium as the standard material. The amount of sample was about 10 mg in all the experiments, and each temperature scan was repeated for six successive cycles.

The DMA measurements were performed by Q800 (TA Instruments, USA), with apparatus compliance of less than 0.2 μm N^{-1} as determined by a prior instrument calibration in tension mode. The tests were carried out in tension mode, using sinusoidal stress with a frequency of 2 Hz and amplitude of 5 μm. The temperature was ramped from 30 to 150 °C at a ramping rate of 5 °C/min. From the measurements, we could determine the storage modulus E', that describes the elastic response to the deformation, the loss modulus E'' that describes the plastic response to the deformation, and the ratio $\tan\delta = E''/E'$, a measure of the damping behavior responsible for determining the occurrence of molecular mobility transitions such as the glass transition.

Isothermal creep test were also carried out in tension mode at constant temperature of 30 °C and maintaining a constant load of 2 MPa for 10 min during the displacement, whereas the subsequent recovery period after load removal was 20 min long. Stress relaxation measurements were performed at constant strain of 0.02% for 10 min, starting from an initial load of 0.001 N.

The FTIR spectra were acquired by VERTEX 70 (Bruker, USA), in the range of 400–4000 cm^{-1}. The samples were analyzed in attenuated total reflection configuration, with an aperture diameter of 3 mm and a spectral resolution of 4 cm^{-1}. For an optimal signal-to-noise ratio, 50 scans were averaged per sample spectrum, and apodized by applying the Blackman-Harris 3-term correction for the Fourier transformation. The interferograms were corrected using a zero-filling factor of 2. All the spectra were baseline-corrected by third-order polynomial and were normalized thereafter.

Results and discussion

Thermal behavior

Figure 1a shows the DSC heating curves of six cycles for the as received PMMA powder, vertically shifted with respect to each other for the sake of clarity, from the bottom to the top. A wide endothermic peak appears in the first heating cycle at ~72 °C. This peak can be ascribed to water absorbed by the PMMA because of the hygroscopic nature of the material; as expected, it disappears in the subsequent heating cycle, due to the release of the adsorbed water moisture. In all the six curves, a peak corresponding to the glass transition temperature (T_g) of PMMA appears, which starts from T_g ~98.2 and undergoes a slight increase on the subsequent cycles of up to ΔT_g ~4.2 °C, probably approaching a plateau since the amount of increase on the successive cycles is progressively decreasing. This effect is due to the condensed structure of the polymer, which spontaneously reassembles into a slightly more stable configuration after each heating cycle.

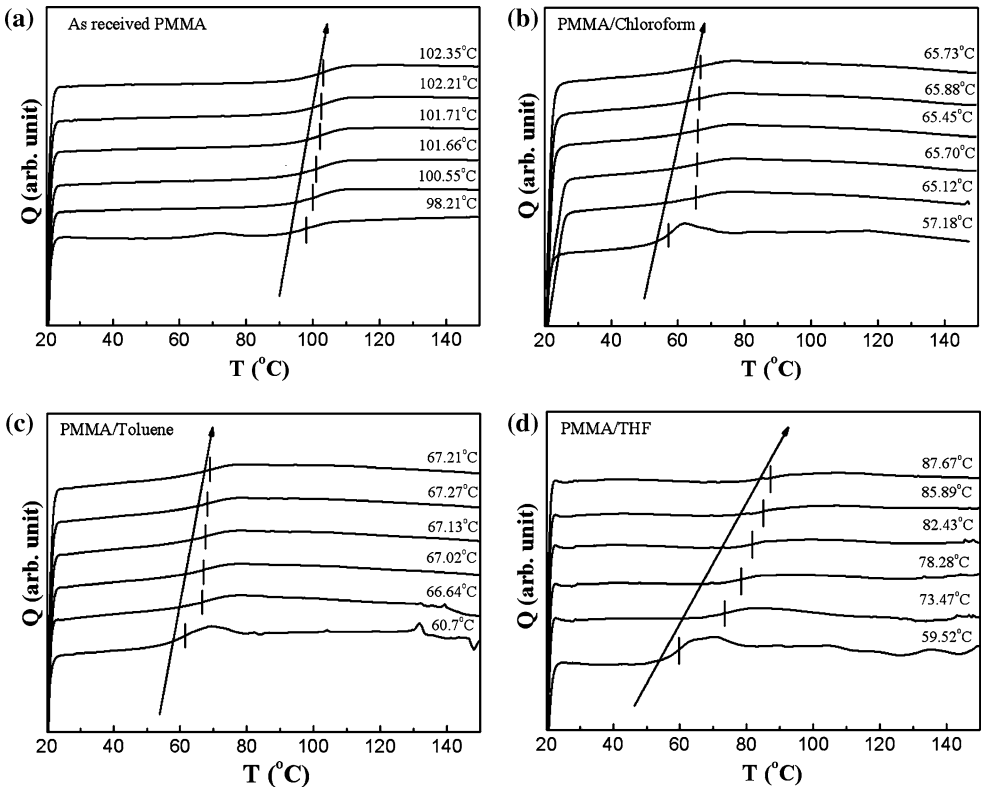

Fig. 1 DSC curves acquired in six successive heat-exchange cycles, for **a** as received PMMA powders, and PMMA films prepared from the different solvents considered: **b** chloroform, **c** toluene, and **d** THF

One common feature of all the PMMA/solvent measurements (Figs. 1b–d) is a significant difference in T_g between the first DSC scan and the subsequent ones, which is not the case for the PMMA powder in Fig. 1a. The first possible reason for this is that the structure of the condensed state of the polymer is affected by the interaction of its molecules with the solvent molecules used in the original liquid phase. A second reason can be the presence of residual solvent in the dried polymer. A third reason can finally be that during solvent processing the polymer chains become distorted. Accordingly, it is evident that the compatibility of the solvent with the particular polymer plays an important role.

In Fig. 1b the same curves are shown for the PMMA/chloroform sample. The glass transition temperature appearing in each heating cycle of Fig. 1b is the lowest (at same cycle number) among all the four cases considered here (Fig. 1a: PMMA powder, Fig. 1c: PMMA/toluene, Fig. 1d: PMMA/THF). The lowest starting T_g observed on the first cycle ($T_g \sim 57.2$ °C) and the overall low increase in T_g during the subsequent cycles in Fig. 1b ($\Delta T_g \sim 8.5$ °C) are due to the strong interactions between the PMMA macromolecules and the Cl atoms of chloroform. This clearly indicates the presence of residual solvent inside the polymer, which did not evaporate from the sample at room temperature, as it would probably be the case with more volatile solvents. It is reasonable to think that on performing the DSC cycles, during heating at the highest temperatures chloroform molecules occluded inside the PMMA film are activated, and chlorine atoms react with polymer macro radicals trapped in the solid polymer matrix with restricted molecular mobility, finally escaping from the polymer cage.

In Fig. 1c the DSC analysis of a PMMA/toluene sample is presented. Similar to PMMA/chloroform (Fig. 1b), the first cycle exhibits a glass transition at much lower temperature than PMMA powder ($T_g \sim 60.7$ °C), with a subsequent low increase ($\Delta T_g \sim 6.5$ °C). In addition, in the first curve some more features appear at much higher temperatures ($\sim$140 °C). These features are weak and irregular shaped, and are probably due to the relaxation of internal stresses in PMMA occurring on removal of most of the residual solvent during the first heating cycle. Both these features and the weaker increase in T_g between the subsequent scans are probably associated with a weaker interaction between residual toluene molecules and PMMA with respect to the case of chloroform. This result is supported by the value of R_a distance of PMMA from the different solvents in the Hansen space of solubility parameters [11, 12], which is larger for toluene ($\sim$10.7 $MPa^{0.5}$) than for chloroform ($\sim$7.8 $MPa^{0.5}$).

Finally, In Fig. 1d the results of similar measurement on a PMMA/THF sample are shown. Compared to the PMMA/toluene sample (Fig. 1c) exothermic irregular features appear also at high temperature in the first heating curve, even though less marked. The starting T_g is also

lower than for PMMA powder ($T_g \sim 59.5$ °C). However, the subsequent increase is much higher than for chloroform and toluene ($\Delta T_g \sim 27.2$ °C), even if still quite lower than for the PMMA powder (final PMMA/THF $T_g \sim 87.7$ °C instead of final PMMA powder $T_g \sim 102.4$ °C, and also lower than the initial PMMA powder $T_g \sim 98.2$ °C). This means that the lowering effect of the solvent on the T_g of PMMA is weaker for the less volatile and polar solvent (i.e., THF with respect to both chloroform and toluene).

Dynamic mechanical behavior

DMA results are expressed by three main parameters, namely the loss modulus E'' that describes the plastic response to the deformation, the storage modulus E', that describes the elastic response to the deformation, and the ratio thereof, $\tan\delta = E''/E'$, a measure of the damping behavior responsible for determining the occurrence of molecular mobility transitions such as the glass transition.

In Fig. 2a the storage modulus E' decreases monotonously with the temperature for all the PMMA samples. The intermediate 70–90 °C region where E' decreases most drastically is obviously related to the PMMA transition from the glassy to the rubbery state. However, among the PMMA/solvent samples, at each temperature in the transition region E' is lowest for PMMA/chloroform (black curve), highest for PMMA/THF, and intermediate between the two for PMMA/toluene. In particular, the relative difference between PMMA/THF and PMMA/toluene is moderate, with a maximum of +0.2 GPa (+25%) for THF at ~77 °C, whereas PMMA/chloroform performs significantly worse from a mechanical point of view, with a maximum difference with respect to PMMA/toluene of −0.56 GPa (−44%) at ~73 °C. Obviously the solvent has a strong effect on the elastic properties of the PMMA. The difference in storage modulus E' is marked around the glass transition and is roughly proportional to the polar nature of the solvent, as this determines the solvent ability to hold the polymer chain intact around this critical temperature.

In Fig. 2b one can see that the loss modulus E'' of the PMMA samples undergoes an increase for all the solvents at intermediate temperatures, and reaches a maximum immediately below the T_g values observed in Fig. 1. On further temperature increase, E″ decreases rapidly towards zero, as the highest temperatures are in all cases well above the respective T_g. At the maximum, the E″ values are even higher than at room temperature, providing an increase with respect to the starting cycle temperature of +1% at 78.3 °C, +9% at 71.8 °C, and +19% at 79.2 °C for chloroform, toluene, and THF, respectively. Again, the highest

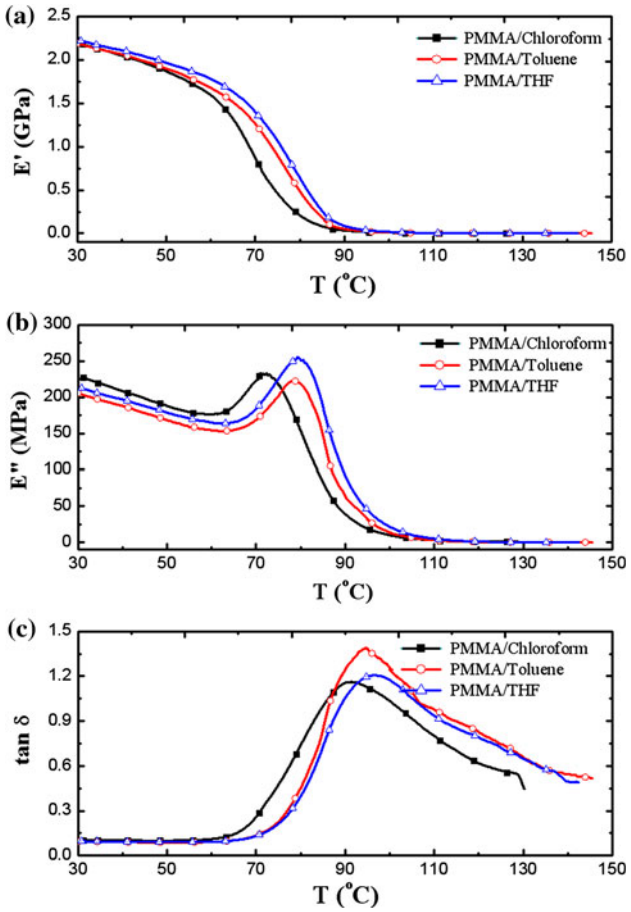

Fig. 2 Variation of **a** storage modulus E' **b** loss modulus E'', and **c** damping factor $\tan\delta$ as a function of the temperature for PMMA film prepared from different solvents

enhancement is obtained for THF, which also occurs at the highest temperature.

Figure 2c finally shows the variation of $\tan\delta$ as a function of the temperature for the PMMA films obtained from different solvents. The peak in the $\tan\delta$ curves for toluene and THF appears at significantly higher temperatures with respect to the case of chloroform, which means that, as already observed in Fig. 1, the PMMA T_g for these samples is less shifted to lower temperatures. The reason is probably a hindering of molecular motion due to stronger bond formation, steric hindrance, and end group rotation. Furthermore, it is found that the value of $\tan\delta$ around the T_g region of maximum slope on the low temperature side of the peak is lower for the PMMA/THF and PMMA/chloroform samples with respect to the PMMA/toluene, and the curves broaden in the vicinity of the peak. Finally, at the highest temperatures the $\tan\delta$ values are noisy and affected by calculation artifacts, since both E' and E'' are quite close to zero and the ratio $\tan\delta = E''/E'$ is therefore not properly defined.

Creep behavior and stress relaxation

Figure 3a shows the short-term creep tests performed on PMMA prepared with different solvents. It is noticed that the creep compliance is lowest for PMMA prepared from THF, as expected. On the contrary, creep strain is highest for PMMA prepared from chloroform and toluene, indicating a softening of the PMMA due to a reduction in stiffness of the entangled network of the polymer chains. With PMMA from THF, the creep strain decreases, with the largest reduction. Overall, the PMMA/THF presents lower creep strain than both the PMMA/chloroform and the PMMA/toluene. Of the PMMA tested from different solvents, PMMA/chloroform performed the worst, having the highest creep strain. The PMMA/toluene provided the second highest creep strain, and PMMA/THF performed the best, having the lowest strain. Figure 3a shows the comparison of the creep compliance for all the samples. Creep compliance for the different solvents of PMMA is in the order of THF < toluene < chloroform.

Figure 3b shows the time behavior of the ratio between the total stress σ and the stress due to creep σ_o over a period of 10 min, corresponding to the upper level state in Fig. 3a. This plot describes the short-term stress relaxation occurring in PMMA prepared with different solvents, and allows describing the residual elasticity of the material when the viscous flow is complete. The plots show that the stress-relaxation modulus σ/σ_o is lowest for PMMA/chloroform system and highest for PMMA/THF system, which therefore appear as the less and the most elastic system, respectively.

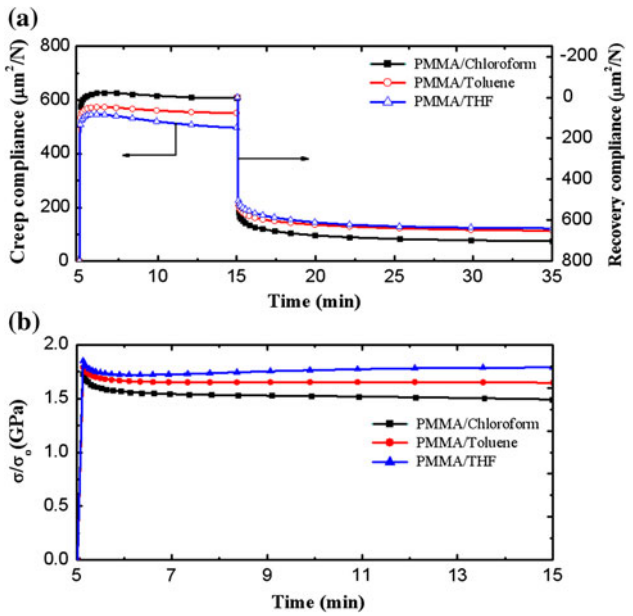

Fig. 3 Experimental **a** creep-recovery compliance and **b** stress-relaxation curves of PMMA samples prepared from different solvents, as a function of the time

This sequence is the same as observed for the storage modulus E′ in Fig. 2a. However, in this case at the final time of 10 min the spacing of both the systems with the PMMA/toluene one is approximately the same, whereas in Fig. 2a PMMA/chloroform seems much worse than both PMMA/toluene and PMMA/THF. Therefore, part of the less desirable mechanical behavior of the PMMA/chloroform system can be assigned to a time dependent transient (see the differences between the curves around 5.5 min, more closely resembling Fig. 2a).

FTIR analysis

Figure 4a–c shows in the main window the room temperature FTIR spectra of the PMMA powder, the bare solvent (in black), and the PMMA sample prepared from the solvent.

In the PMMA spectrum the following characteristic features appear due to the polymer structure: the stretching peak of C=O in carbonyl group PMMA at 1725 cm^{-1}; the peaks of the bend vibration of $–CH_2$ and $–CH_3$ group of PMMA at 1450 and 1388 cm^{-1}, respectively; the peaks of the stretching vibration of the C–O–C and C–H group PMMA at 1100–1200 cm^{-1} and 3000–2840 cm^{-1}, respectively, [13].

Furthermore, several more peaks can be found due to the possible different tacticities of PMMA. In particular, the three absorption peaks at 751, 910, and 1063 $cm^{-1}$are attributed to the syndiotactic PMMA structure [14]. However, the steric hindrance of the substituted group $–COOCH_3$ on the PMMA chain makes the C–C in the end of growing chain rotate, which is helpful to form syndiotactic and atactic structures.

Figure 4a shows the FTIR spectra for the PMMA/chloroform sample. A close-up of the carbonyl band centered at 1725 cm^{-1} is shown in the inset. It can be seen that at 1700 cm^{-1} a weak shoulder (see arrow) appears inside the band of the PMMA/chloroform sample with respect to the PMMA powder. This is due to the hydrogen bonding contribution directly to the carbonyl fraction. However, this does not affect the band center position.

Figure 4b shows the FTIR spectra for the PMMA/toluene sample. In this case, as shown in the inset, close to the PMMA syndiotactic peak at 751 cm^{-1} two new peaks appear in the toluene-casted PMMA at $\sim$733 and $\sim$696 cm^{-1}, as a result of the interaction between toluene and PMMA. Compared to the original peaks in the toluene, the peaks in PMMA/toluene are shifted toward higher wavenumbers, probably due to molecular movement and group rotation. Furthermore, the PMMA powder band at 2848 cm^{-1} in the figure main window is shifted to 2872 cm^{-1}. This can be a consequence of the steric hindrance effect, which is higher for toluene, thus leading to

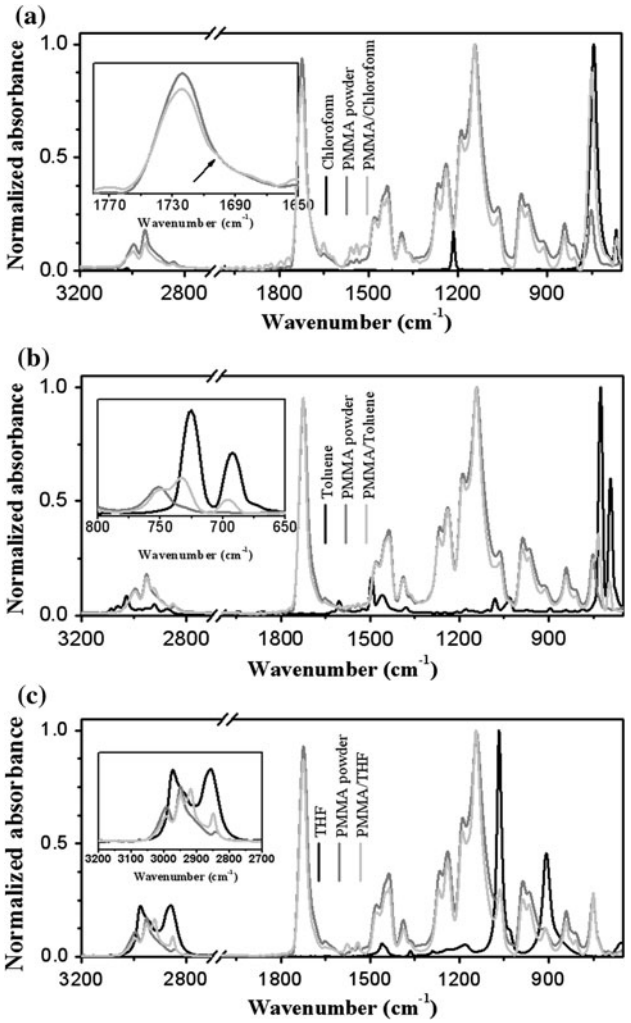

Fig. 4 FTIR spectra of the PMMA powder and, for each panel, bare solvent, and PMMA/solvent sample, for **a** chloroform, **b** toluene, and **c** THF, respectively. The *insets* show close-up PMMA of peculiar spectral regions

hindering the molecular interactions inside the PMMA chains.

Figure 4c shows the FTIR spectra for the PMMA/THF sample. In this case, as shown in the inset, one new peaks appear in the THF casted PMMA at $\sim 2920\ \mathrm{cm}^{-1}$ as a result of the interaction between THF and PMMA probably due to methyl moieties being attached by hydrogen bonding.

The overall knowledge of the thermal and elastic properties resulting upon use of a given solvent could be of practical application in smart nanocomposite coatings based on functional nanocrystals fed into the respective polymer solutions, which could have consequences both during manufacturing (e.g., by means of hot-embossing) and during later operation (e.g., working at high-ambient temperature or under tough contact wear conditions due to a high number of operation cycles).

Conclusion

In this study the effect of using chloroform, toluene, and THF as the solvent in the preparation of PMMA films drop casted from concentrated solutions has been addressed. The thermomechanical properties of the PMMA samples appear to be strongly influenced by the choice of the solvent used for the preparation, due to its polarity and to its capability of forming H-bonds with the polymer. The dynamic mechanical, creep-recovery and stress relaxation behavior of the PMMA films prepared from three different solvents has been studied. Overall, the best performing solvent appears to be THF for all cases. The optimization of the thermomechanical properties of these films is of interest in devices based on nanocomposites, such as organic light emitting diodes, biochemical sensors or other functional coatings.

References

1. Haller I, Hatzakis M, Srinivasan R (1968) IBM J Res Develop 12:251
2. Burke B, Herlihy T Jr, Spisak A, Williams K (2008) Nanotechnology 19:215301
3. Chou SY, Krauss PR, Renstrom PJ (1995) Appl Phys Lett 67:3114
4. D'Amore F, Lanata M, Pietralunga S, Gallazzi M, Zerbi G (2004) Opt Mater 24:661
5. Sciancalepore C, Cassano T, Curri M, Mecerreyes D, Valentini A, Agostiano A, Tommasi R, Striccoli M (2008) Nanotechnology 19:205705
6. Bistac S, Schultz J (1997) Int J Adhesion Adhesives 17:197
7. Feng X, Weiwen F, Rongshi C (2006) Chem China 1:45
8. Hong PD, Huang HT, Chou CM (2000) Polym Int 49:407
9. Bubb DM, Papantonakis M, Collins B, Brookes E, Wood J, Gurudas U (2007) Chem Phys Lett 448:194
10. Kaczmarek H, Chaberska H (2008) Polym Testing 27:736
11. Patra N, Barone AC, Salerno M (2011) Adv Polym Technol 30:12
12. Hansen C (2007) Hansen solubility parameters: a user's handbook, 2nd edn. CRC Press, Boca Raton, FL
13. Vien DL, Colthup NB, Fateley WG, Grasselli JG (1991) Infrared and Raman characteristic frequencies of organic molecules. Academic Press, New York
14. Brandrup J, Immergut EH (1999) Polymer handbook, 4th edn. Wiley Interscience, New York